

Detecting Functional Relationships between Simultaneous Time Series

C.L. Goodridge, L.M. Pecora, T.L. Carroll, and F.J. Rachford
Code 6345, US Naval Research Lab, Washington, DC 20375

We describe a method to characterize the predictability and functionality between two simultaneously generated time series. This nonlinear method requires minimal assumptions and can be applied to data measured either from coupled systems or from different positions on a spatially extended system. This analysis generates a function statistic, ρ_{c^0} , that quantifies the level of predictability between two time series. We illustrate the utility of this procedure by presenting results from a computer simulation and two experimental systems.

PACS number(s): 05.10.-a, 05.45.-a, 05.45.Tp

1. INTRODUCTION

A common challenge encountered by experimentalists in nonlinear dynamics is how to relate pairs of time series, such as those measured from two points on a spatially extended system or from two coupled systems. Many nonlinear systems exhibit spatial as well as temporal dynamics and an understanding of the spatial behavior is often vital to understanding the overall dynamics [1]. Examples of such spatiotemporal systems are “auto-oscillations” of magneto-static spin wave modes in ferrimagnetic films [2], the response of a magnetostrictive ribbon to AC magnetic fields, and fluid motion in Taylor-Coquette flow [3] or Rayleigh-Bernard Convection [4]. One way to characterize the spatial dynamics is to simultaneously monitor a property of the system at two different positions and determine the relationship between the resulting data. The relationship between simultaneous time series may also describe properties of the coupling between two coupled systems. A wide variety of linear techniques are available to investigate the functionality between concurrent time series, but these techniques often fail to provide any useful information if the relationship is nonlinear.

In this paper we will describe a general nonlinear technique that investigates the functionality between pairs of time series with minimal assumptions about the nature of either the data or the dynamics. This generality allows this technique to be applied to a wide range of experimental systems and to account for more general functionality than strictly linear. The result of this analysis is a function statistic, ρ_{c^0} , that quantifies the predictability and functionality between the two time series and can be compared to results from linear techniques such as the cross-correlation. This technique may be useful to experimentalists with time series data as well as provide another tool for general time series analysts.

The procedure builds on techniques designed to investigate functionality between time series [5], especially those of several of the authors [6,7]. These earlier procedures calculate a statistic that quantifies certain properties of functions relating time series such as continuity or differentiability. This analysis provides a way to calculate a function statistic that is a measure of the predictability between the time series. Roughly speaking, this statistic quantifies how well can we predict the behavior of one time series if we know the behavior of the other time series. This technique can be extended to investigate the nature of the functional relationship between the two time series by testing for nonlinearity in the function. One important aspect of this technique is that it uses the data to establish a limiting length scale--a limit of relevance [8]--rather than intuition or knowledge about the system and is applicable to both experimental and computational results.

2. PROCEDURE

Given two simultaneous time series $\{h_i, g_i\}$ [9], we construct vectors \mathbf{x}_i and \mathbf{y}_i and attractors \mathbf{X} and \mathbf{Y} , such that $\mathbf{x}_i = (h_i, h_{i+1}, \dots, h_{i+(d-1)})$ and $\mathbf{y}_i = (g_i, g_{i+1}, \dots, g_{i+(d-1)})$ by time delay embedding. The parameters of the embedding, the time delay and the embedding dimension d , are determined using the minimum of autocorrelation function [1] and the false nearest neighbor algorithm of Kennel and Abarbanel [10], respectively [11]. However, any combination of d and τ that adequately captures the dynamics of the system should yield useful results. Next we assume that a function F exists such that $\mathbf{y}_i = F(\mathbf{x}_i)$. Function F is assumed to be continuous but no other conditions are imposed. Since the determination of F may not be trivial, an intermediate goal is to investigate properties of the function. We will calculate a function statistic that allows us to describe whether function F actually exists, how accurately we can make predictions between time series, and if the function is nonlinear. To derive this statistic, we assume that nearby points on \mathbf{X} map to nearby points on \mathbf{Y} (see Fig. 1), provided F exists. This behavior is equivalent to the two time series being related by a continuous function. Our function statistic, ρ_0 , is a measure of the local predictability between the two time series. A high value indicates strong predictability between the time series.

Here is an outline of the procedure to calculate ρ_0 . In all of the following, we assume that we have measured the data in such a way that h_i and g_i are sampled simultaneously and we define \mathbf{x}_i and \mathbf{y}_i as corresponding points if the indices of the first coordinates are equal. We systematically investigate clusters of nearest neighbors on one attractor (the source), and quantify the locality of the corresponding points on the other

attractor (the target). Each cluster of points on the target attractor will yield a value for c^0 . We repeat this calculation for a number of clusters and average the values to find an attractor wide value for the function statistic. In order to characterize the locality of the points on the target, we need a reference length scale r . We utilize the variance of points on the attractors as our measurement and quantify the strength of the predictability using the significance of this variance. The significance of the variance is defined as the probability that the actual variance is larger than a given value, assuming σ^2 is the mean variance. This value will be calculated using a probability distribution function for the variance. There are two primary steps in this analysis, first, determine the reference length scale and then calculate of the function statistic. The two steps are outlined below:

- I. Determination of length scale r on Target Attractor
 1. Select a point (a “center”) y_0 on the target attractor.
 2. Gather N nearest neighbors of this center, where N is large enough to achieve good statistics but small enough to calculate a minimum length scale (Fig. 2).
 3. Determine the variance of these points.
 4. Set the significance of the variance equal 0.95 and solve for $r(y_0)$.
 5. Repeat for a number of other centers and average values to find attractor wide r .
- II. Determination of Function Statistic
 1. Select a center x_0 on source attractor.
 2. Gather all of the points within some radius r of this center.
 3. Find all of the corresponding (i.e. simultaneous in time [12]) points on the target attractor (Fig. 3).
 4. Find the variance of these points and calculate the significance of this variance $c^0(x_0)$.
 5. Vary r to maximize the significance for this point.
 6. Repeat for a number of other centers and average to find a value for the function statistic.

For good predictability our null hypothesis is that r is a typical length scale for our data, implying that sets with no functional relationship will have predictability errors $\gg r$, hence resulting in low significance of variance. In actuality, we want to show that the variance is much smaller than r^2 and that r acts as a good upper bound so we know prediction at error levels below r is likely. This is the same as requiring that the variance of a cluster of points has an upper bound. High values of the significance of the variance correspond to high predictability and therefore the high likelihood that the time series are related by a function.

A. Derivation of Significance of Variance

In order to calculate the significance of the variance for these clusters of points, we need an expression for the probability distribution function (PDF) for the variance, which we will determine using the central limit theorem. For any group of values, $\{s^2_1, s^2_2, s^2_3, \dots\}$,

where both the mean $\sigma^2 = \frac{1}{N} \sum_{i=0}^{N-1} s^2_i$ and the standard deviation $\gamma^2 = \langle (s^2_i - \langle s^2 \rangle)^2 \rangle$ are

known, we can approximate the PDF(s^2) as $\exp -\frac{N(s^2 - \sigma^2)^2}{2\gamma^2}$ as $N \rightarrow \infty$. If the

Gaussian Approximation ($\gamma^2 = 2\sigma^4$) is applied, then the probability distribution function can be written as

$$PDF(s^2) = \exp -\frac{N}{4} \left(\frac{s^2}{\sigma^2} - 1 \right)^2 \quad (1).$$

We then use this expression as the probability distribution function of the variance of clusters of points on attractors. The significance of the variance is defined as the probability that a given variance is larger than s^2

$$signf(var) = 1 - \frac{1}{norm} \int_0^{var} \exp -\frac{N}{4} \left(\frac{s^2}{\sigma^2} - 1 \right)^2 ds^2, \quad (2)$$

where $norm$ is the normalization constant (Fig. 4). This expression is used to calculate both the length scale ℓ_c and the function statistic ℓ_{c0} (see previous section).

When using a Gaussian for the probability distribution function of a set of variances, we need to account for the possibility of unphysical negative variances. We account for this by integrating from 0 to var , truncating the negative variances, and by modifying the normalization constant. If the mean of the distribution is far from 0, then $norm \approx 2$. On the other hand, as the mean of the distribution approaches 0, then $norm \approx 1$. To find the normalization constant, we set

$$\frac{1}{norm} \int_0^{var} \exp -\frac{N}{4} \left(\frac{s^2}{\sigma^2} - 1 \right)^2 ds^2 = 1 \text{ as } var \rightarrow \infty \quad (3)$$

to find that $norm = 1 + \text{erf} \frac{\sqrt{N}}{2}$, erf is the error function. This expression for the normalization constant accounts for the truncation of negative variance values.

B. Scale Determination

One strength of this analysis is that we calculate a length scale from the data itself without making any assumptions about the dynamics. The attractors allow us to determine a scale directly from the data. Here is the procedure. Select a randomly determined point \mathbf{y}_0 (the center) on the target attractor $\{\mathbf{y} \mid \mathbf{y}_0, \mathbf{y}_1, \mathbf{y}_2, \mathbf{y}_3, \dots\}$. Gather the N nearest neighbors of center \mathbf{y}_0 and calculate the variance of these points,

$$\text{var} = \frac{1}{N-1} \sum_{j=1}^N (y_j - \bar{y})^2 \quad (4),$$

where \bar{y} is the mean. A Theiler Exclusion [13] is used to avoid counting points that are very close in time as nearest neighbors. Each cluster of points will contain a specified number of points, large enough to achieve good statistics but small enough to produce a minimum length scale. The number of points N has ranged from 20-50 points to 1-2% of the total number of points, depending on the nature of the data (considering factors such as noise and the total number of points).

To determine a value for σ , we insert this variance into the equation for the significance of the variance, set the significance equal to 0.95 and determine the corresponding σ . Repeat for a number of randomly determined centers (typically 100) and average the values to produce an attractor-wide scale σ ,

$$\sigma = \frac{1}{N_c} \sum_{i=1}^{N_c} \sigma(\mathbf{y}_i) \quad (5).$$

The resulting value is based solely on the data itself without any a priori assumptions about the system dynamics. We now use this scale to calculate the function statistic.

C. Calculation of Function Statistic

Given scale σ on the target attractor, we now turn to the source attractor $\{\mathbf{x} \mid \mathbf{x}_0, \mathbf{x}_1, \mathbf{x}_2, \mathbf{x}_3, \dots\}$. To begin the function statistic calculation, we gather all of the points within some radius δ , $\{\mathbf{x}_0 \mid \mathbf{x}_1, \mathbf{x}_2, \mathbf{x}_3, \dots\}$, of some randomly selected center on this attractor \mathbf{x}_0 . (In this case the indices of these points refer to the spatial neighbors of \mathbf{x}_0 , not the temporal order of the time series.) The variance and significance of the corresponding points on the target attractor $\{\mathbf{y}_0 \mid \mathbf{y}_1, \mathbf{y}_2, \mathbf{y}_3, \dots\}$ are then calculated. δ is then varied on the source attractor (Fig. 5) to maximize the $\text{signf}(\text{var})$ for this center,

$$c_0(\mathbf{x}_0) = \max_{\delta} \{\text{signf}(\mathbf{x}_0)\} \quad (6).$$

The function statistic c^0 is defined as the average of the maximum values for the $\text{signf}(\text{var})$ for a number of clusters across the attractor:

$$c^0 = \frac{1}{N_c} \sum_{i=1}^{N_c} c^0(\mathbf{x}_i) \quad (7),$$

N_c is the number of centers, usually around 100[14]. This is roughly a measure of the percentage of points on the first attractor whose corresponding points fall within the neighborhood of \mathbf{y}_0 on the target attractor. High values indicate that good predictability and strong functionality, low values that it is unlikely that the two time series are related by a function.

D. Function Statistic beyond Linear

Another application of this analysis is to use this statistic to test for nonlinearity in the functional relationship between two time series. The function statistic beyond linear is a measure of how much more accurate a nonlinear prediction is than a strictly linear prediction. The procedure for this application is this:

1. Fit the attractors to a linear model: $\mathbf{Y} = \mathbf{AX}$. We have used a least squares fit model.
 2. Determine the variance of the residues
- $$\eta = \frac{1}{N} \sum_{i=1}^N (y_i - Ax_i)^2 \quad (8).$$
3. Use this value η for the scale σ in the significance calculation.

If there is only a linear relationship between the two attractors, η is on the same order as the values for the function statistic beyond linear are low. If there are nonlinear components to the relationship between the time series, then $\eta > \sigma$ and the values for the function statistic are high. Care must be taken when using this analysis and should only be interpreted as such when there is some relationship between the two time series. Two completely stochastic time series will produce a large value for the variance of the residues and the calculated statistic may also be high. We now present data from several experimental systems:

2. ROSSLER FORCED LORENZ SIMULATION

We will first apply this technique to data from a computer simulation to verify that we get results that are expected. We will use a six-dimensional system consisting of a Lorenz system driven by a Rossler system:

$$\begin{aligned}
& \dot{X}_R = -(Y_R + Z_R) \\
\text{Rossler-Drive} \quad & \dot{Y}_R = X_R + aY_R \\
& \dot{Z}_R = b + Z_R(X_R - c) \\
& \dot{X}_L = -\sigma(X_L - Y_L) \\
\text{Lorenz-Response} \quad & \dot{Y}_L = -X_L Z_L + \rho X_L - Y_L + K(\gamma Y_R - Y_L), \text{ K = coupling constant} \\
& \dot{Z}_L = X_L Y_L - \beta Z_L
\end{aligned} \tag{9}, \tag{10}$$

where $a=b=0.2$, $c=0.7$, $\sigma=10$, $\rho=8/3$, and $\beta=60$. In order to make the two systems

comparable we select $K=3.0$ as gain constant, which makes the Rossler amplitude

comparable to the Lorenz amplitude and tune the time steps to make the two time scales

comparable. We present three sets of data where we determine the predictability from the Rössler time series to the Lorenz time series. The data are simultaneous measurements of the Rossler X coordinate and the Lorenz X coordinate. The first set has no additive noise and no coupling, the second set has no additive noise and strong coupling, and the third set has 5% additive noise and strong coupling. Values for the cross-correlation, function statistic, and function statistic beyond linear for each of these states is shown in Fig. 6. The cross-correlation and the function statistic are low for the uncoupled case, which is consistent for two independent systems. The lack of any linear relationship implies a large value for the variance of the residues and explains the higher value for the function statistic beyond linear.

The high values for the three statistics indicate that the two time series have strong predictability and are strongly related by a function for the two coupled cases. The addition of 5% noise has a very slight (one or two percent change) effect on the two statistics. The high value for the function statistic beyond linear for both coupled cases indicate that the function relating the two time series may have nonlinear components.

3. SPIN WAVES IN YTTRIUM IRON GARNET FILMS

A solid state system that exhibits spatial-temporal chaotic dynamics is spin wave modulation of resonant modes in Yttrium Iron Garnet (YIG) films. YIG is a technologically useful ferrimagnetic material used in microwave devices such as limiters, resonators, and filters and many aspects of its nonlinear behavior have been studied and exploited [15]. A number of previous experiments performed by several of the authors [16-19] have investigated the global temporal dynamics of YIG sample structures. In these experiments,

we analyze the response at two positions on the surface of a YIG film to investigate the spatial dynamics across YIG films.

When YIG films are placed in saturating DC magnetic fields, the atomic spins initially align and precess around the direction of the DC field. Unless the spins are excited by an AC magnetic field, the spin precessions will damp out. When a resonant AC magnetic field is applied perpendicular to the DC field, the spins will precess around the DC field direction at the resonant frequency [20]. Phase modulations in the processions of neighboring spins produce traveling spin waves which, when reflected at the film boundaries, result in standing waves corresponding to the magneto-static modes of the film. At low applied AC powers, these modes are linear at the resonant frequency but are coupled to initially negligible nonlinear modes. As the excitation power is increased above a threshold power (the Suhl Instability)[15], the linear modes begin to interact with continuum half-frequency spin waves in the film. The non-linear interaction of the stationary modes and the half frequency spin wave manifold produce nonlinearities that eventually dominate the dynamics. These interactions lead to low frequency (kHz) modulations of the amplitude of the (GHz) magneto-static mode resonances. These modulations have been observed in both small spheres and thin films of YIG. These modulations are measured in our experiments and can exhibit periodic (called auto-oscillations), quasi-periodic, and chaotic behavior.

A diagram of the experiment can be seen in Fig. 7. Our sample is a rectangular film cut from a single YIG crystal with dimensions $0.85 \times 0.72 \text{ cm}^2$ and is 37 microns thick. The modulations of the magneto-static modes are detected by using a pair of coaxial probes mounted near the film surface. The film is mounted in a wave guide and is excited by a 2-4 GHz microwave field. The probes are oriented to pick up the resonant oscillation of the magnetization in the film. The probe microwave field is amplified and detected using standard diode detectors. The kHz auto-oscillation modulation is then digitized and processed. Both periodic and chaotic states have been observed over a wide parameter range. Each data set consists of a time series of the voltage signal from each probe. We investigate the relationship between the two time series by initially performing cross-correlation analysis to quantify the linear aspects of the relationship and then investigating the nonlinear aspects using the function statistic.

Figure 8 shows the linear correlation and nonlinear function statistic as a function of microwave excitation power for a power sweep at performed at 460.1 Oe and 3.0251 GHz. Initially the signal to noise ratio is low but eventually the system evolves into a region of periodic states where both the cross-correlation and function statistic values are high. Both statistics are determined using 100 centers for both the scale and function statistic

calculations. Both measures drop off as the states lose periodic structure and become more chaotic. We also show a plot of the function statistic beyond linear (Fig. 9), calculated using a least squares approximation for the linear model. The high value for the function statistic beyond linear indicates that the error in the linear model is greater than the attractor wide noise scale. These results imply that there is a nonlinear component to the relationship in this parameter range.

We present results from another power sweep (performed at 2.9747 GHz and 449.9 Oe) in Fig. 10. The states in this power sweep produce periodic signals with similar spectra except in the region between 5.4 and 7.4 dBm. Here, the measured time series are quasi-periodic with two non-commensurate frequencies. The individual probes measure both frequencies but the relative intensities of the individual frequencies are different for each probe. The higher frequencies are more intense at the position monitored by the first probe, while the lower frequencies dominate the dynamics at the position monitored by the second probe. At these powers, the linear cross-correlation is much lower than the values for either of the nonlinear statistics. This implies that there is some functionality in the power range that is highly nonlinear in nature. This is also an example of a system with functionality that can not be characterized by the linear cross-correlation and demonstrates the utility of the function statistic analysis. In order to further explore the behavior in this power range, we calculated both the function statistic and function statistic beyond linear for these states interchanging the source and target attractors. These values were very close to those previously determined (both for the function statistic and the function statistic beyond linear) and support the existence of an invertible function relating the time series.

We would like to determine if the results in Fig. 10 are caused by differences in the dynamics as driving power is increased or by different noise levels in the time series used to calculate the statistics. As a test of the noise level, we use the Gamma statistic [21]. To find the Gamma statistic, we calculate the mean square distance from an arbitrary reference point to the p 'th nearest neighbor in the \mathbf{X} attractor ($\Delta(p)$) and the mean square distance from an arbitrary reference point to the p 'th nearest neighbor in the \mathbf{Y} attractor ($\gamma(p)$). We then plot $\gamma(p)$ as a function of $\Delta(p)$. As $p \rightarrow 0$, Steffansson and Jones show that $\gamma(p)$ approaches the variance of the noise level in the g time series. We can estimate the variance of the noise level from the intercept of the $\gamma(p)$ vs $\Delta(p)$ plot and the variance of the residues for a least squares linear model in Fig. 11. We plot the value of the statistic as defined above, which

is a measure of the noise variance in the g time series. We also plot σ_g , which is a measure of the variance of a group of near neighbors on the \mathbf{Y} attractor (calculated when we determine the function statistic). The σ_g statistic remains roughly the same size over the range of powers in Fig. 11, indicating that the noise levels in the different time series are roughly the same relative to the signal size. The differences seen between the statistics in Fig. 10 are not caused by differing noise levels. It is interesting to note that σ_g is roughly the same size as σ_x ; and the two different methods of determining a minimum length scale on the attractor \mathbf{Y} give similar results. σ_g (calculated in the determination of the function statistic) is upper bounded by σ_x , indicating that this noise statistics is smaller than the underlying noise level in the data.

4. MAGNETOSTRICTIVE RIBBON EXPERIMENT

We also applied the statistics described above to data from an experiment involving a magnetostrictive metal ribbon. We suspended a ribbon of Metglass 2605sc between a pair of Helmholtz coils. The top of the ribbon was rigidly clamped, while a 1.6 g mass was clamped across the bottom of the ribbon, allowing the bottom of the ribbon to swing freely. The ribbon was 25 mm wide, 60 mm long, and 1 mil thick. The Helmholtz coils produced a magnetic field in the plane of the ribbon. The magnetic field consisted of a 6.5 Oe DC field and an AC field that could be set to different magnitude and frequencies. The AC magnetic field coupled to domain walls in the ribbon to exert a time varying force on the ribbon. Figure 12 is a simple diagram of the experiment.

Two small spots (about 1 mm^2) on the ribbon were illuminated by a He-Ne laser. The ribbon surface was not smooth, so the spots produced diffuse reflections. The reflected light was focused on two small-area differential diode detectors, which compared the reflected beams to reference beams straight out of the laser in order to reduce noise from laser intensity modulations (noise). Movement of the reflected beam across the detector produced a time varying signal proportional to the deflection of the ribbon at the spot illuminated by that spot. One laser spot was kept fixed in the center of the ribbon, while the other spot was scanned over the surface, so that two different signals were produced by the two detectors. Because each of the beams hit the ribbon at a different angle, different signals were produced even when both beams illuminated the same position.

The magnetization of the ribbon was coupled to its strain because the ribbon had a large magnetostriction. A magnetic field applied to the ribbon would change the stiffness of the ribbon, as well as changing its shape. The stiffness of the ribbon affected its mechanical

response, so driving the ribbon with an AC magnetic field produced a highly nonlinear system.

We applied the function statistic, the function statistic beyond linear, and linear cross-correlation to pairs of time series from the ribbon. Because the motion of the ribbon was highly nonlinear, it was not possible to tell by eye what the relation was (if any) between the two time series. Instead, we applied the statistic to determine what sort of relationships there might be. We drove the ribbon at an AC frequency of 113 Hz, which is the location of a bending mode of the ribbon. We then sampled the time series signals from the two detectors every time the driving signal crossed zero in the positive direction. We applied the statistics to these strobed time series.

A. Driving at 1.4 Oe

Figure 13 shows the power spectrum of one of these strobed time series when the AC magnetic field RMS amplitude was 1.4 Oe. Figure 14 is a Poincare section obtained by plotting the strobed time series from one detector against the strobed time series from the other detector. The response of the ribbon appears to be quasiperiodic, responding at frequencies of 113 Hz, 4.5 Hz, and combinations of the two frequencies.

In order to determine statistics, the laser spot that generated the time series labeled “y” was fixed at the center of the ribbon, while the time series labeled “x” was scanned over the ribbon. There were 8 scans recorded along the narrow dimension of the ribbon and 32 scans recorded along the long dimension, for a total of 256 scans.

Figure 15(a) is a plot of the function statistic beyond linear c_0 obtained by comparing the strobed time series from the center of the ribbon to the strobed time series at other points at the ribbon. Each time series contained 2000 points embedded in 5 dimensions. White on the plot indicates a value of 1, while black indicates a value of 0. c_0 is near 1 over the entire surface of the ribbon, indicating that the relationship between the two embedded time series is not explained by a linear map. Either the relationship is nonlinear or there is no relation between the time series.

Figure 15(b) shows the value of the function statistic c_0 over the surface of the ribbon (where 1 of the time series is taken at the center of the ribbon). c_0 is slightly larger near the middle of the ribbon than near the ends, which suggests that it is easier to predict the motion at a point on the ribbon from a nearby point than from a distant point. We expect that we should be able to predict the motion of one point on the ribbon from the motion at another point because the ribbon is undergoing quasiperiodic motion, but noise can reduce the value of c_0 .

Figure 15(c) shows the maximum value of the cross correlation between the time series from the center of the ribbon and time series at other points. The cross correlation measures whether or not two signals are linearly related, but it also allows for a shift in time. The cross correlation between the time series is not very large for most points on the ribbon, so while c_0 shows that there is some predictability between time series from different points on the ribbon, the relationship between these time series is not simply linear. The cross correlation agrees with the function statistic beyond linear c_0 , which shows that any relation between time series is nonlinear.

B. Driving at 6.1 Oe

Figure 16 shows a power spectrum from a strobed time series when the AC magnetic field had an RMS amplitude of 6.1 Oe. Spectral lines at multiples of 5 Hz are still present, but there is now also a large broad band background signal. In Fig 17, the Poincare section for this data no longer appears to be quasiperiodic. The statistics for pairs of time series were computed as before, with an embedding dimension of 5.

The function statistic beyond linear c_0 in Fig. 18(a) is near 1 everywhere, suggesting that any relation between motion on different points on the ribbon is nonlinear. The function statistic c_0 in Fig. 18(b) appears to show two separate regions. c_0 is near 0 for regions near the top of the ribbon and larger for regions near the bottom. The motion of the top half of the ribbon is not very predictable from the motion of the bottom half. The cross correlation plot in Fig. 18(c) shows that the relation between motion on different parts of the ribbon is very nonlinear, except when the two parts of the ribbon are very close together.

This magnetic ribbon is being driven very hard, so it is unlikely modeling of the motion of the ribbon for such large driving fields would be possible. All the information we can gain about the ribbon will come from statistics such as those used above. It is tempting to speculate whether or not the motion seen when the driving field is at 6.1 Oe is chaotic, but in our experience, attempting to calculate indicators of chaos such as Lyapunov exponents from experimental data are not yet very reliable at distinguishing chaotic motion from other complicated types of motion.

5. Conclusions

We have described a new way of quantifying the relationship between two time series and applied this technique to several experimental systems. This technique allows for the computation of a statistic that describes the strength of the relationship between two time

series and also the intensity of the nonlinearity of any such relationship. Using this technique along with other linear and nonlinear techniques can help elucidate the relationship between time series and the underlying dynamics. Results from a variety of experiments show that the utility of this analysis.

The authors wish to thank D. King, W. Lechner, and J. Valenzi for technical assistance. C.L. Goodridge acknowledges support from an Office of Naval Research/American Society for Engineering Education Fellowship.

1. H. Kantz and T. Schreiber, *Nonlinear Time Series Analysis* (Cambridge University Press, Cambridge, UK, 1997).
2. C. Goodridge, T. Carroll, L. Pecora, et al., Proceedings of the Fifth Experimental Chaos Conference, (1999).
3. A. Aitta, G. Ahlers, and D. S. Cannell, Phys. Rev. Lett. **54**, 673 (1985).
4. M. Dubois and P. Berge, J. Fluid Mech. **85**, 641 (1978).
5. D. T. Kaplan, Phys. D **73**, 38 (1994).
6. L. Pecora, T. Carroll, and J. Heagy, Phys. Rev. E **52**, 3420 (1995).
7. S. Schiff, P. So, T. Chang, et al., Physical Review E **54**, 6708 (1996).
8. The scale or limit of relevance is one possible measure of the stochastic noise level in the data.
9. These measurements can be of position, temperature, voltage or any other measurable quantity of the spatiotemporal system.
10. H. D. I. Abarbanel, *Analysis of Observed Chaotic Data* (Springer-Verlag, New York, 1995).
11. The attractors may have different dimension and time delay parameters
12. We define simultaneous points on the attractors to be vectors with identical first coordinates, since we do not require that the attractors have the same dimension or time delay.
13. J. Theiler, Phys. Rev. A **41**, 3038 (1990).
14. The number of centers is at the discretion of the user of this technique. In our analysis, we have typically used 100 centers.
15. H. Suhl, J. Phys. Chem. Solids **1**, 209 (1957).
16. T. L. Carroll, L. M. Pecora, and F. J. Rachford, Phys. Rev. A **40**, 377 (1989).
17. T. L. Carroll, L. M. Pecora, and F. J. Rachford, IEEE Trans. Magn. **27**, 5441 (1991).
18. D. J. Mar, T. L. Carroll, L. M. Pecora, et al., J. Appl. Phys. **80**, 1878 (1996).
19. D. J. Mar, T. L. Carroll, L. M. Pecora, et al., J. Appl. Phys. **81**, 5734 (1997).
20. B. Lax and K. J. Button, *Microwave Ferrites and Ferrimagnetics* (McGraw-Hill, New York, 1962).
21. A. Stefansson and A. J. Jones, Neural Comp. Appl. **5**, 131 (1997).

Figures

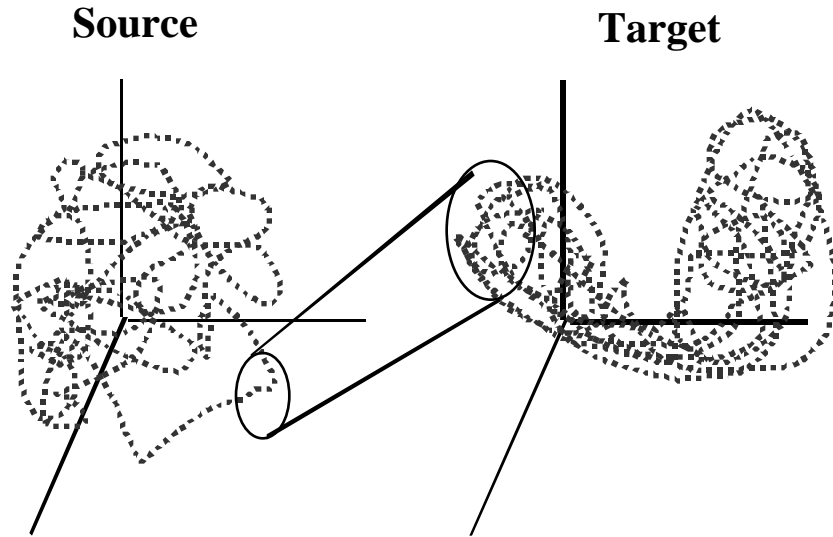


FIG. 1. This technique quantifies the behavior of corresponding points on the two time series; that is, do points, which are nearest neighbors on the source attractor, have corresponding points (simultaneous in time) which are nearest neighbors on the target attractor.

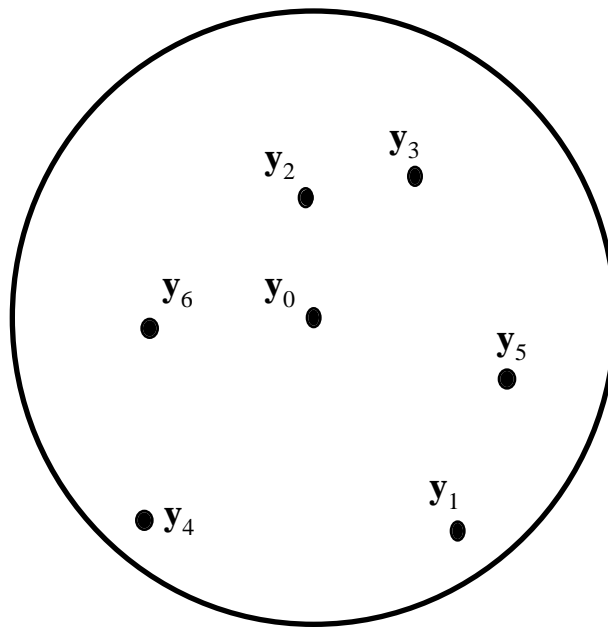


FIG. 2. The target attractor is divided into clusters of points, which are nearest neighbors to a center point. The variance of these points is used in the determination of the length scale

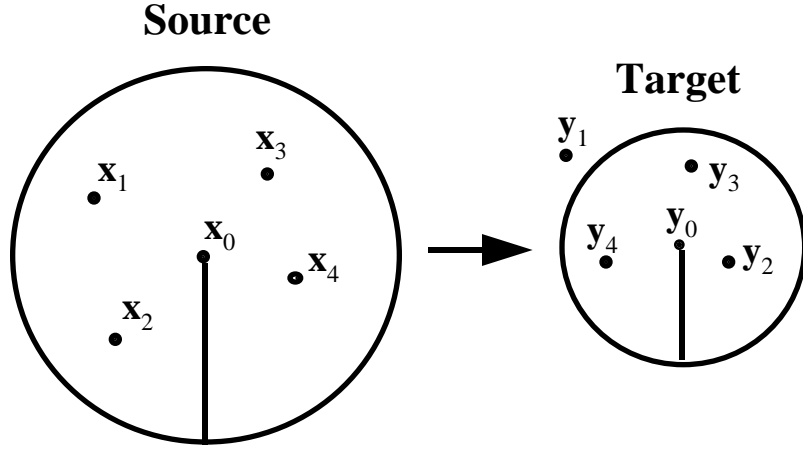


FIG. 3. Nearest neighbors on the source attractor (defined as being within radius r of a given center point X_0) and the corresponding points on the target attractor. Our statistic quantifies the locality of the corresponding points to within some length scale ℓ .

$$PDF(s^2) = \exp \left[-\frac{N}{4} \frac{s^2}{\sigma^2} - 1 \right]^2$$

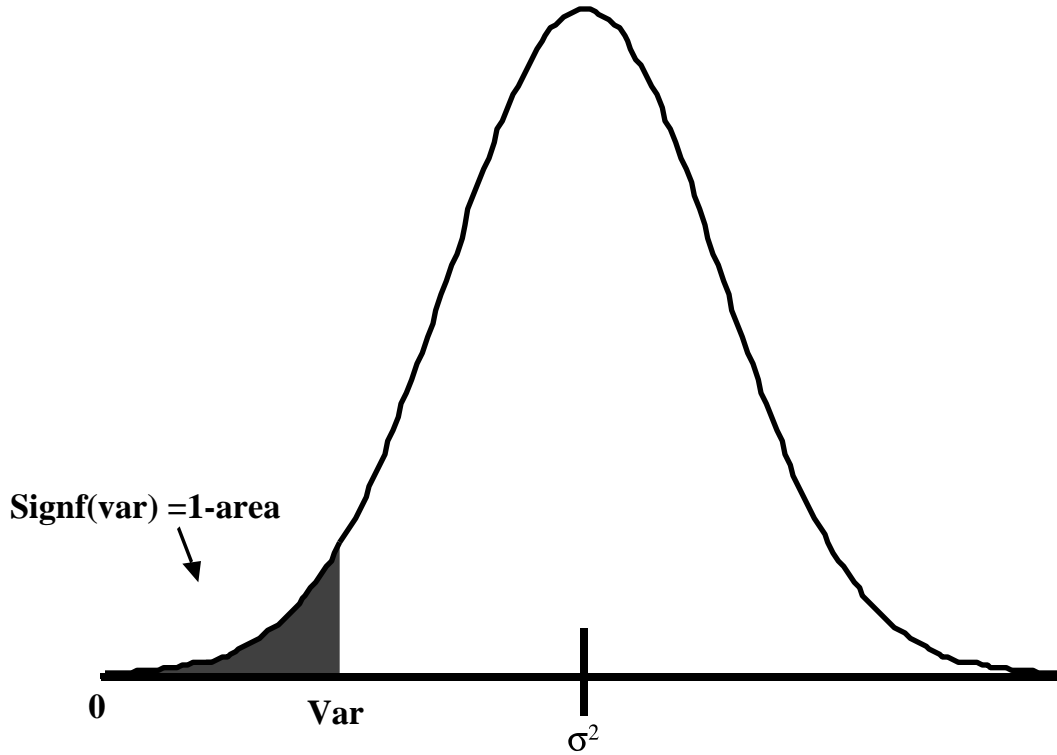


FIG. 4. We evaluate the Gaussian from $0 \rightarrow \text{var}$ to determine a value for the significance of the variance and therefore the function statistic. The normalization of the integration will depend on the mean of the distribution.

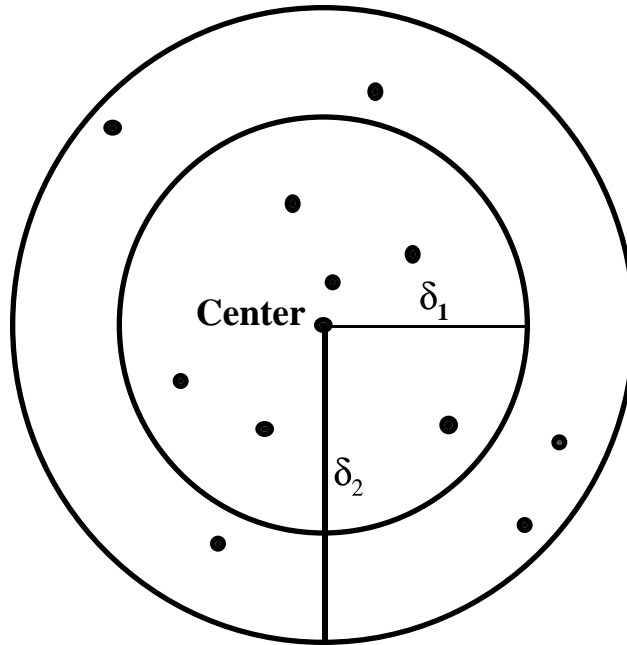


FIG. 5. The radius is varied around a given center and the variance of each collection of points is calculated. The number of points used to determine the length scale varies depending on the nature of data.

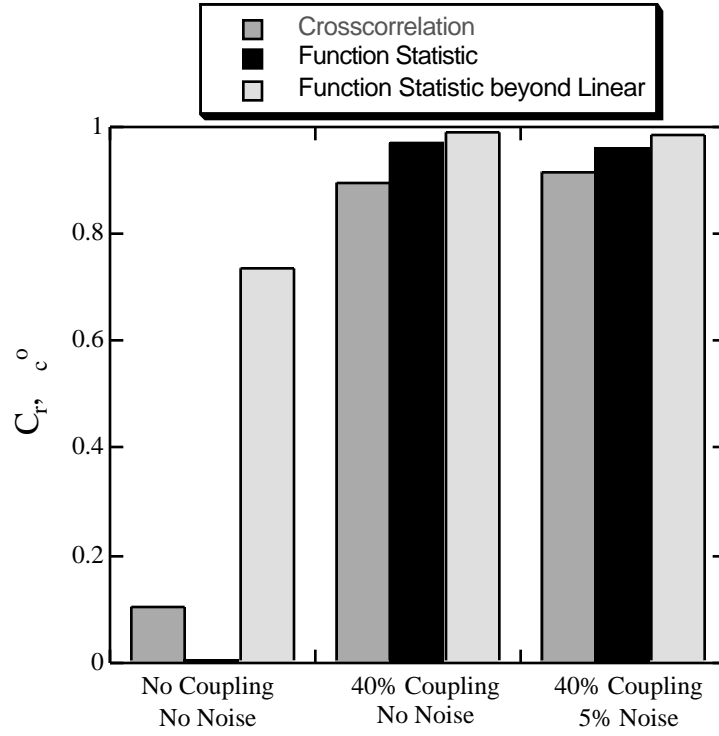


FIG. 6. A plot showing three different statistics, the cross-correlation, the function statistic, and the function statistic beyond linear, for the Rossler driven Lorenz system. The high values for the cases with coupling indicate that there is a functional relationship between the two time series, likely nonlinear in nature considering the high values for the nonlinear statistic.

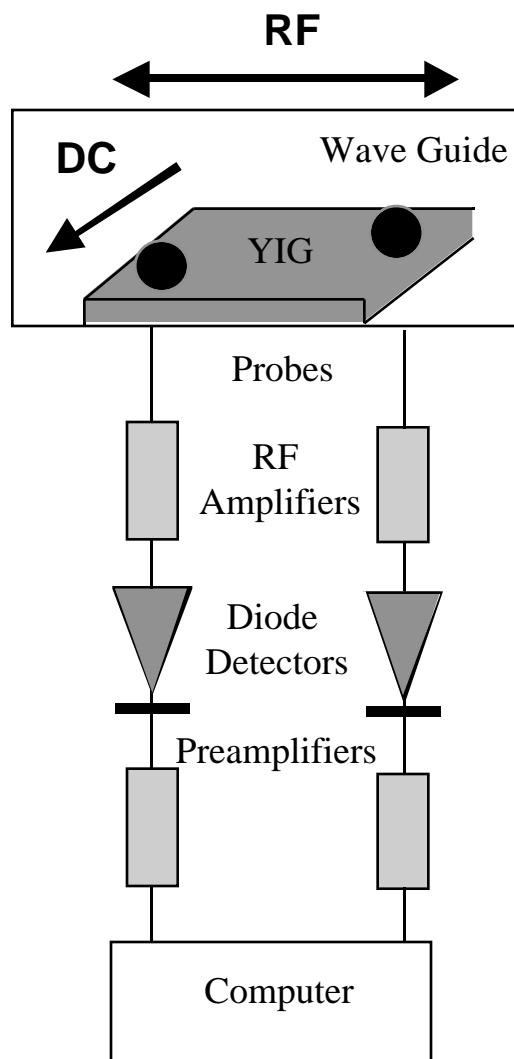


FIG. 7. Coaxial probes measure the magnetic moment of the YIG film at two positions. A pair of diode detectors then detects the modulation of the spin waves.

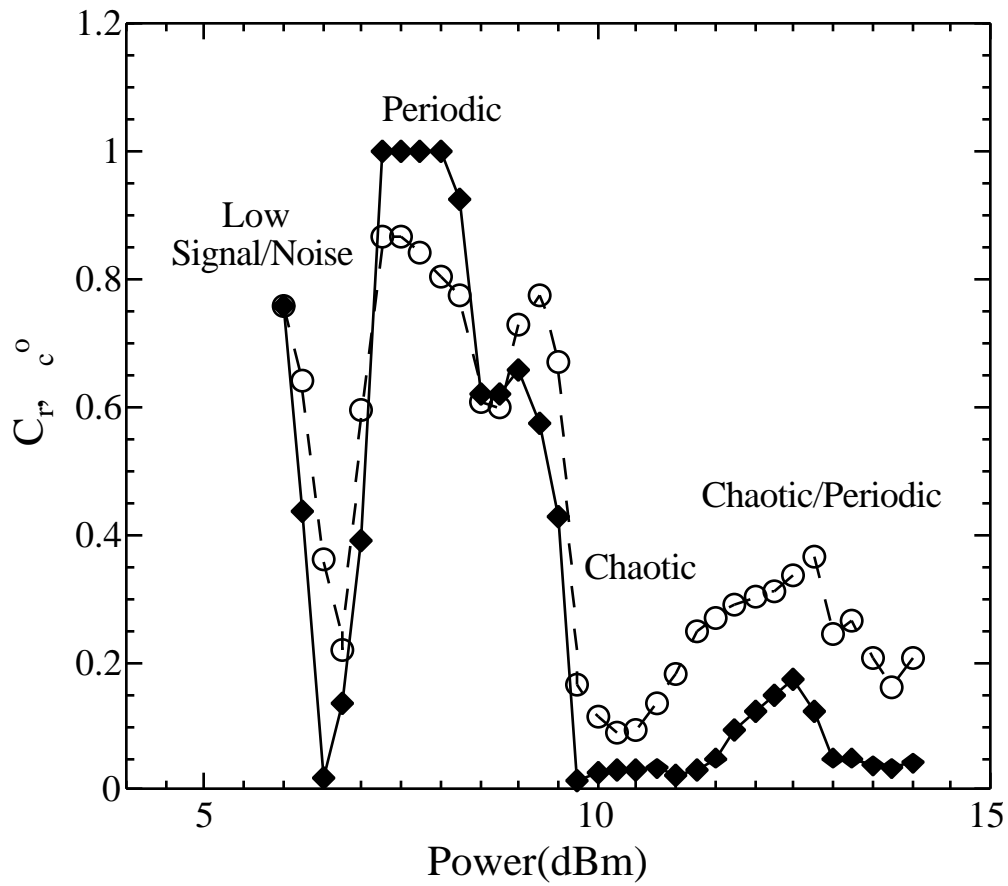


FIG. 8. This plot shows the maximum value for the cross-correlation (O) and the function statistic (◆) for a power sweep performed at DC field 460.1 G and excitation frequency 3.0251 GHz. The linear cross-correlation and the nonlinear function statistic exhibit similar behavior, indicating that, in a region of periodic behavior, there is strong functionality, which drops off as the power is increased.

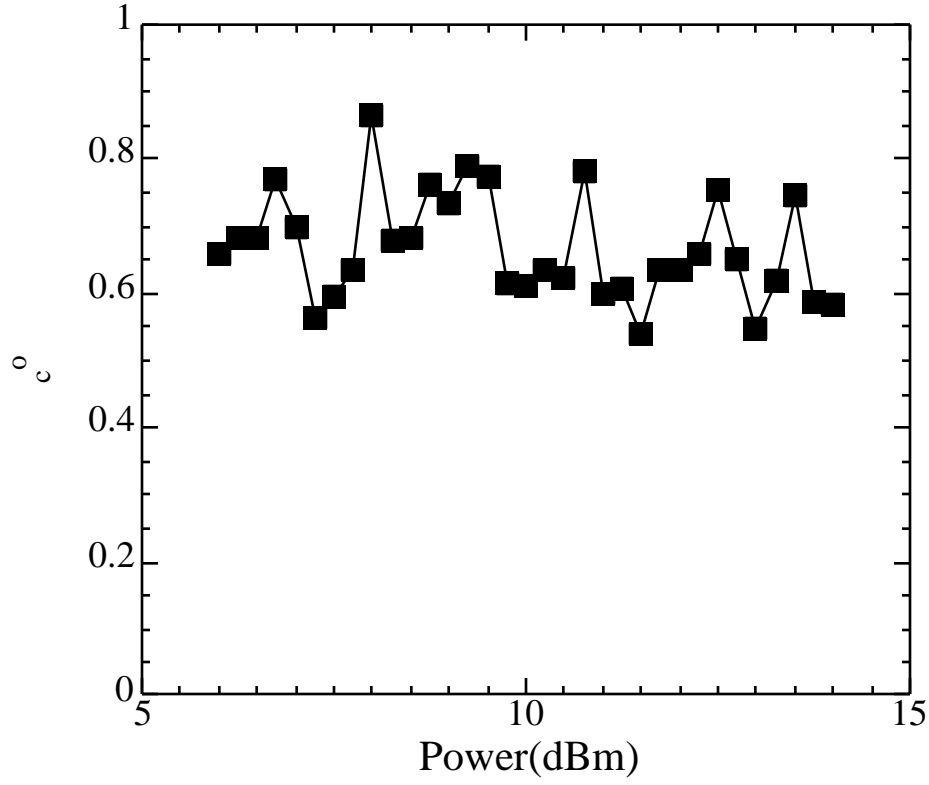


FIG. 9. This plot shows the value of the function statistic beyond linear (■) for the power sweep performed at 460.1 G and 3.0251 GHz. The high values even where both the cross-correlation and function statistic values are low (such as those above 10dBm) indicate that there is some functionality in these states and that it is nonlinear in nature.

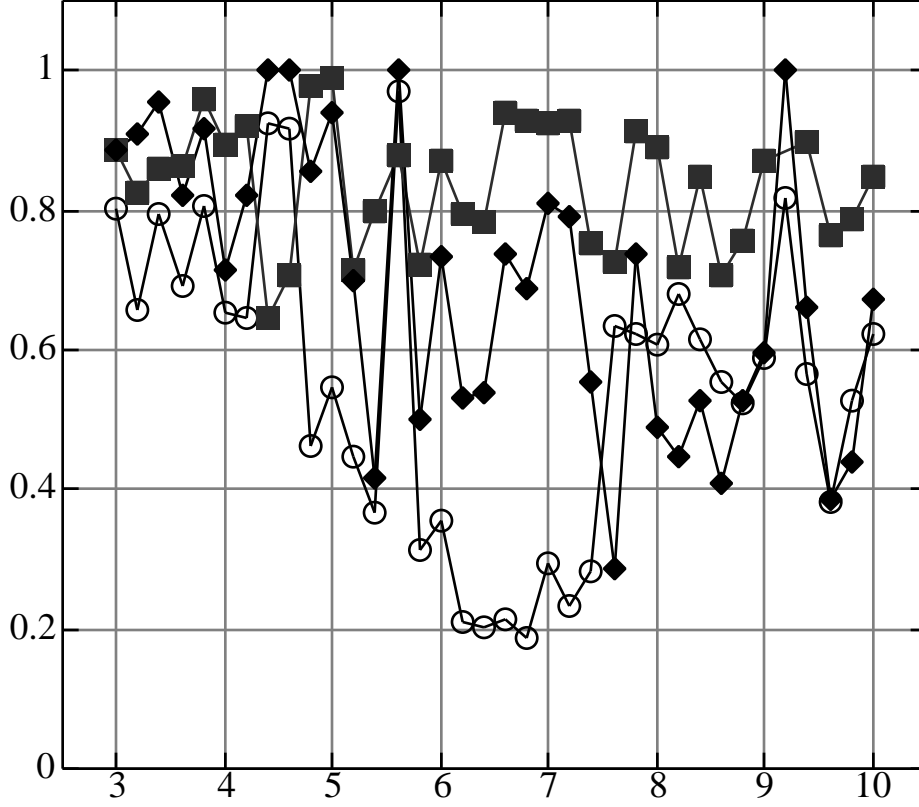


FIG. 10. A plot of the cross-correlation (O), function statistic (◆), and function statistic beyond linear (gray ■) for a power sweep at 2.9747 GHz and 449.9 Oe. In the region between 5.4-7.4 dBm, the two nonlinear statistics are higher than the linear cross-correlation, indicating that the functionality in this region is nonlinear.

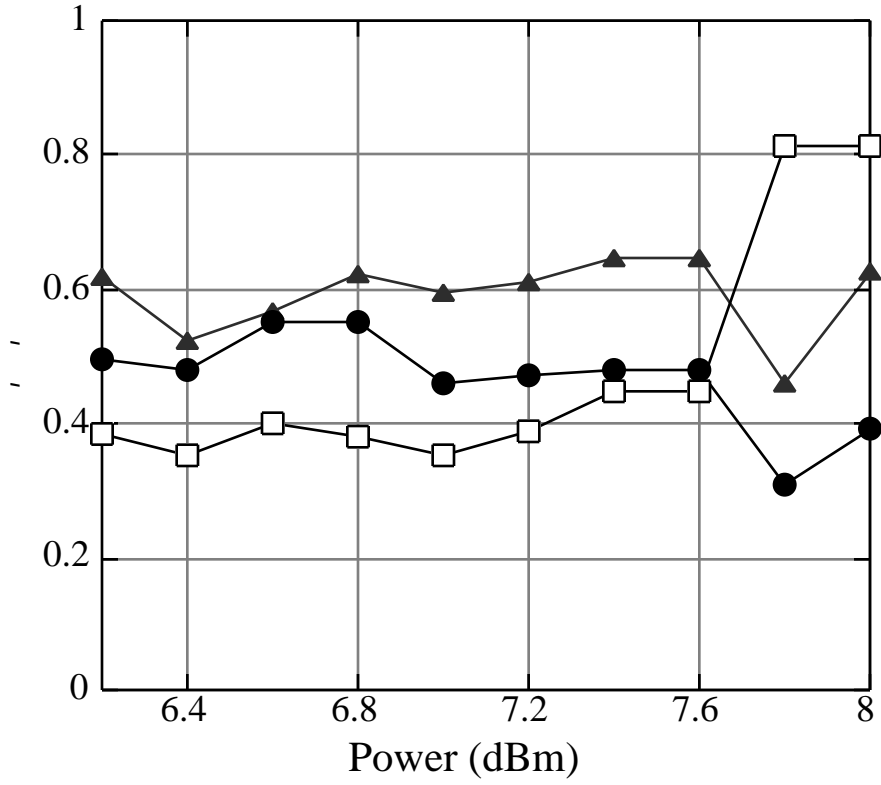


FIG. 11. Plots of two different noise levels: (a measure of the stochastic noise level of the time series data) (\blacktriangle), (found during the calculation of function statistic) (\square), and (the variance of the residues from a least squares linear model) (\bullet). \square is upper bounded by \blacktriangle but the two noise statistics are close in value. \bullet has more variation and is dependent on the strength of a linear fit between the attractors.

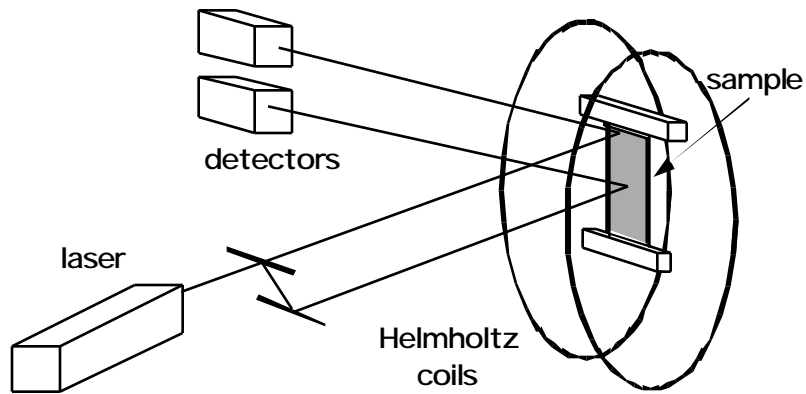


FIG. 12. Simple diagram of the driven magnetic ribbon experiment. The laser illuminates 2 spots on the ribbon, and the motion of these spots is used to detect the motion of the ribbon at the location of the spot.

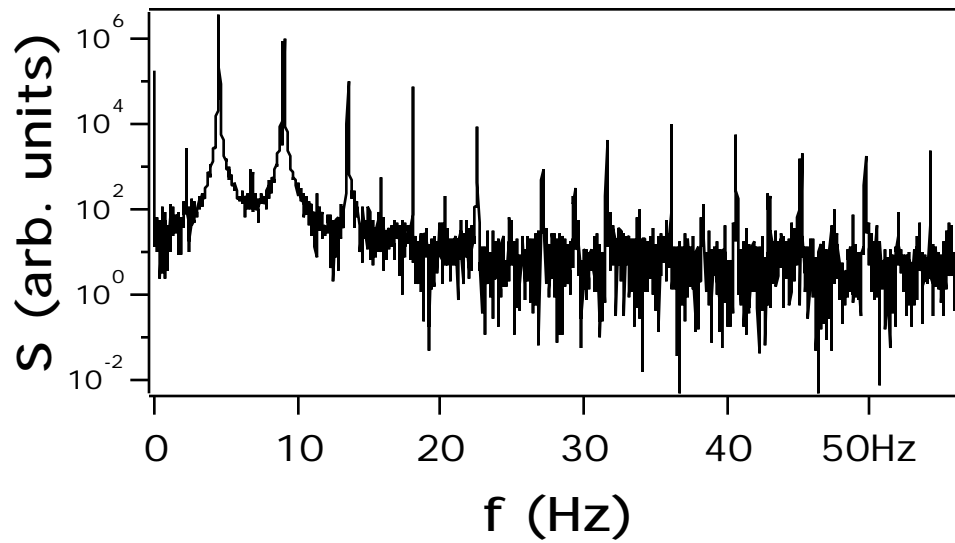


FIG. 13. Power spectrum S of the signal from the center of the ribbon when the AC driving field is 1.4 Oe. The time series has been sampled once per cycle of the driving frequency of 113 Hz.

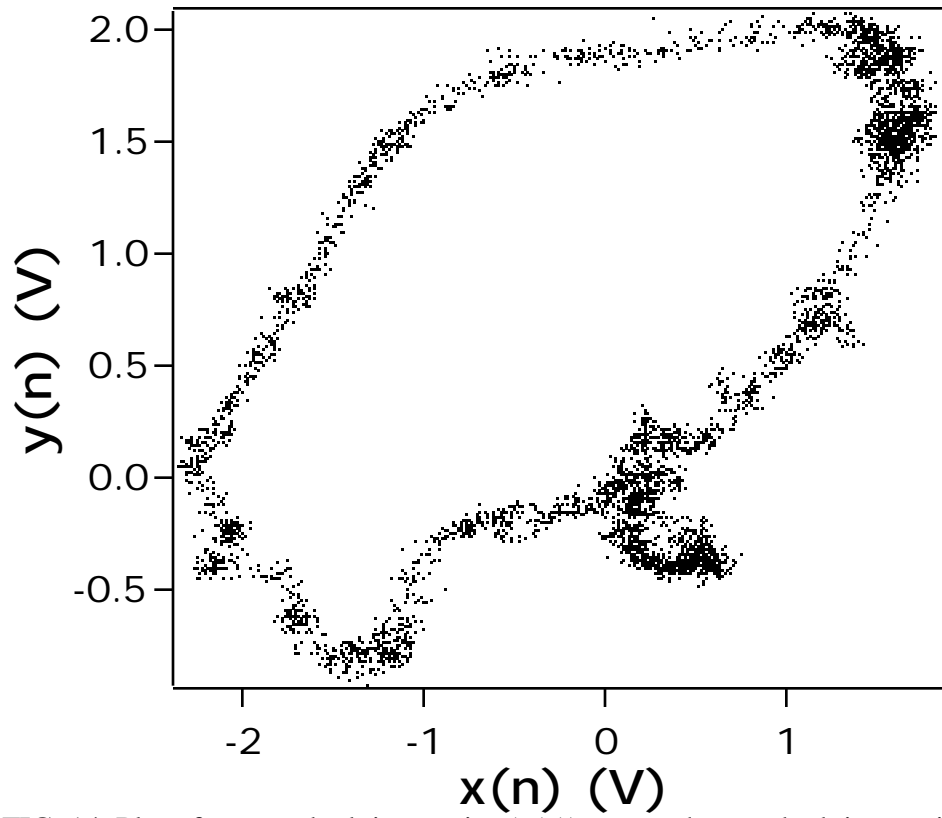


FIG. 14. Plot of one strobbed time series ($x(n)$) vs. another strobbed time series ($y(n)$) taken with both laser spots at the center of the ribbon when the driving amplitude is 1.4 Oe. The 2 laser beams are at different angles, so the two time series are not the same.

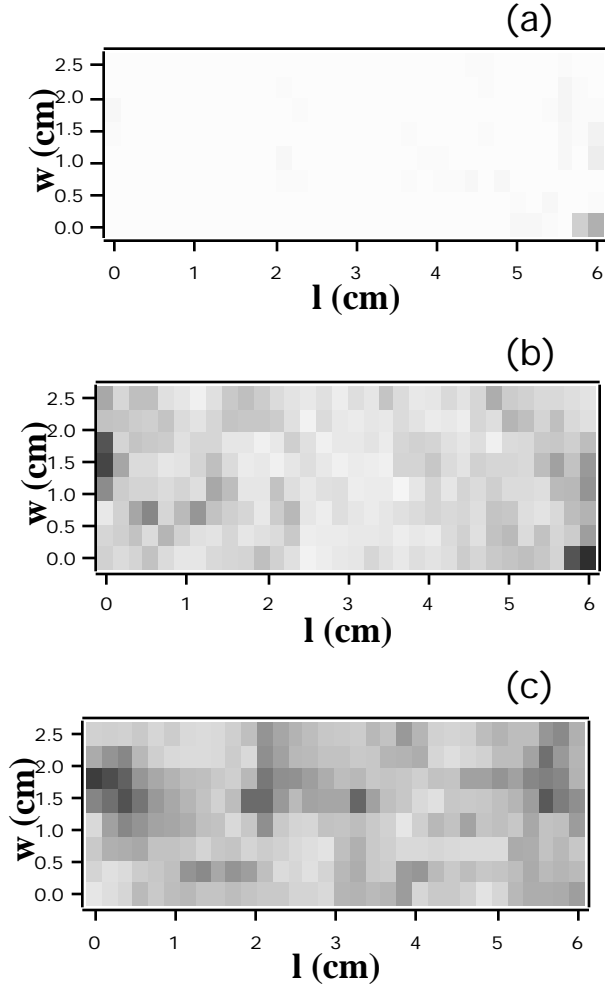


FIG. 15. (a) Plot of the significance beyond linear statistic χ_c^0 over the surface of the ribbon, where one on the time series is from the center of the ribbon (when the drive amplitude is 1.4 Oe). White is equal to 1, while black is equal to 0. (b) Plot of the function statistic χ_c^0 over the surface of the ribbon. (c) Plot of the maximum value of the cross correlation between detected time series from the ribbon.

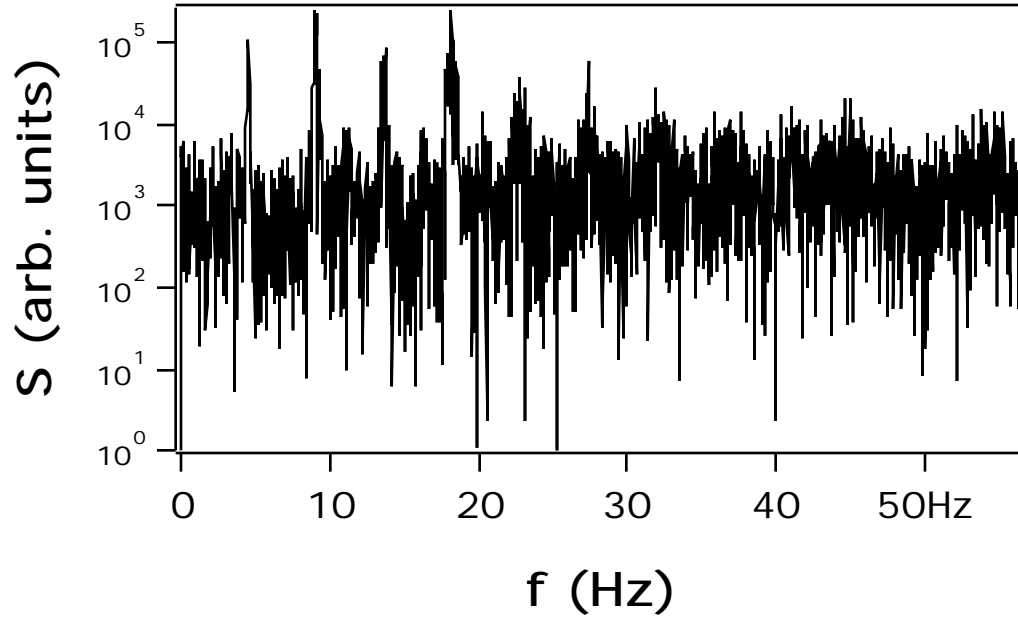


FIG. 16. Power spectrum S of the signal from the center of the ribbon when the AC driving field is 6.1 Oe. The time series has been sampled once per cycle of the driving frequency of 113 Hz.

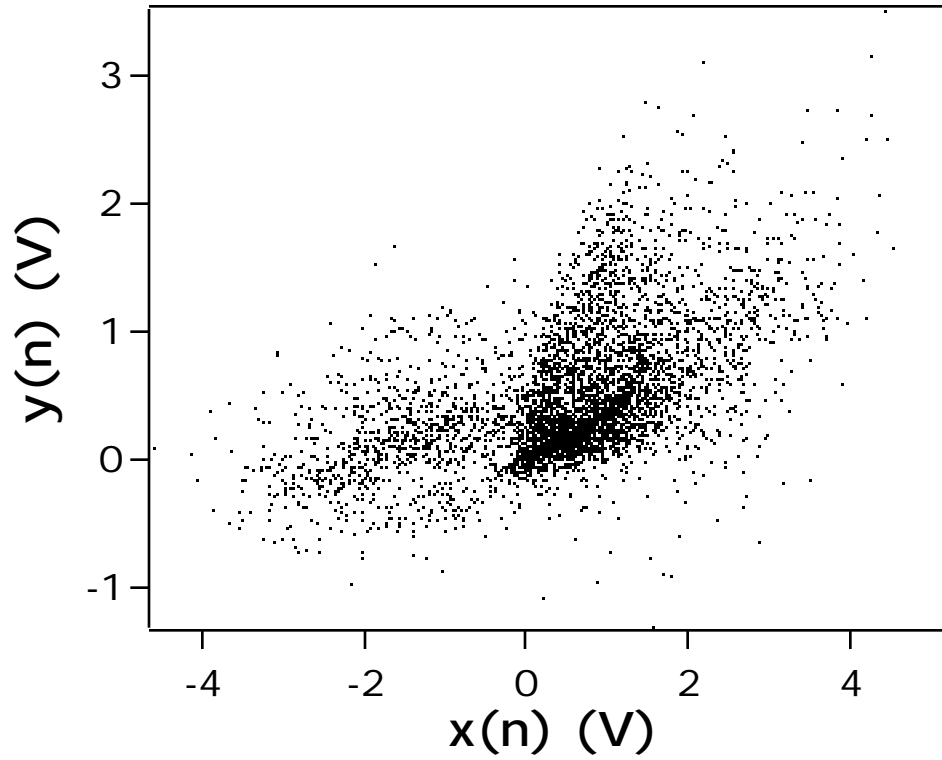


FIG. 17. Plot of one strobed time series ($x(n)$) vs. another strobed time series ($y(n)$) taken with both laser spots at the center of the ribbon when the driving amplitude is 6.1 Oe. The 2 laser beams are at different angles, so the two time series are not the same.

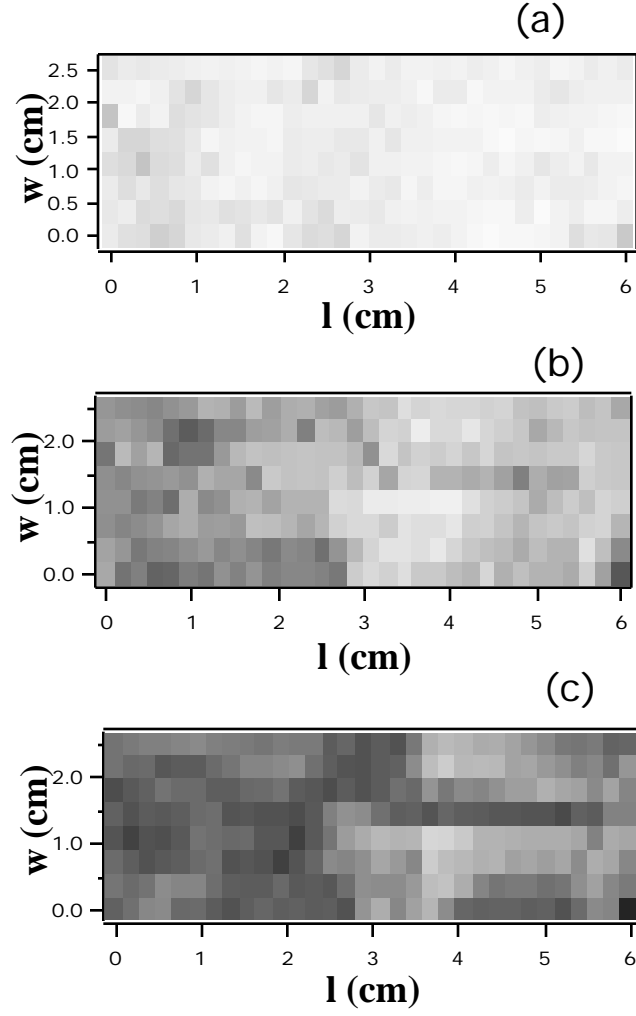


FIG. 18. (a) Plot of the significance beyond linear statistic χ_c^0 over the surface of the ribbon, where one on the time series is from the center of the ribbon (when the drive amplitude is 6.1 Oe). White is equal to 1, while black is equal to 0. (b) Plot of the function statistic χ_c^0 over the surface of the ribbon. (c) Plot of the maximum value of the cross-correlation between detected time series from the ribbon.